Nuclear Science and Techniques (2025) 36:26
https://doi.org/10.1007/s41365-024-01633-9

Properties of the drip-line nucleus and mass relation of mirror nuclei

Meng-Ting Wan[1] · Li Ou[1,2] · Min Liu[1,2] · Ning Wang[1,2]

Received: 3 September 2024 / Revised: 25 November 2024 / Accepted: 29 November 2024 / Published online: 10 January 2025

Abstract
The isospin asymmetry and quadrupole deformation value of drip-line nuclei are investigated using the Weizsäcker–Skyrme nuclear mass formula. We observe that for heavy nuclei at the neutron drip line, the Coulomb energy heightened by an augmented charge could not be mitigated completely by symmetry energy because of isospin asymmetry saturation but is resisted complementally by strong nuclear deformation. The positions of saltation for the difference in proton numbers between two neighboring nuclei at the neutron drip line, and the isospin asymmetry of the neutron drip-line nucleus as a function of the neutron number distinctly correspond to the known magic numbers, which can serve as a reference to verify the undetermined neutron magic number. Through fitting of the binding energy difference between mirror nuclei (BEDbMN), a set of Coulomb energy coefficients with greater accuracy is obtained. A high-precision description of the BEDbMN is useful for accurately determining the experimentally unknown mass of the nucleus close to the proton drip line if the mass of its mirror nucleus is measured experimentally.

Keywords Nuclear mass formula · Drip-line nucleus · Magic number · Mirror nuclei · Coulomb energy

1 Introduction

The nuclear mass is one of the most fundamental properties of the nucleus and is important in many fields of nuclear physics [1]. On the one hand, the nuclear mass can provide important information on the nuclear structure and reactions, such as the nuclear deformation [2], properties of neutron-rich nuclei [3, 4], structure and decay of superheavy nuclei [5–8], shell effect [9–12], nuclear drip line [13], halo nuclei [14], and synthesis of superheavy nuclei [15–18]. On the other hand, the nuclear mass is a key input to many problems in nuclear astrophysics. It has a vital influence on the composition [19] and cooling rate [20] of a neutron star and directly determines the evolution path of the rapid neutron capture process in stellar nucleosynthesis [21–23].

The aforementioned research on nuclear physics requires a high-precision nuclear mass table. With the rapid development of radioactive nuclear beam devices and detection technology, nuclei with measured masses continue to move toward the drip lines. Recently, significant progress has been made in the measurement of short-lived isotope nuclear masses far from stable regions. Approximately 2500 nuclear masses have been measured with an accuracy of less than hundreds of keV [24–27]. However, owing to a series of difficulties in synthesis, separation, and detection in experiments, the nuclei involved in the studies of superheavy islands, drip-line nuclei, nuclear astrophysics, etc., are still significantly beyond the current scope of nuclei with measured masses. No significant breakthroughs may occur in the foreseeable future, particularly on the neutron-rich side. Therefore, a model that can accurately describe known masses and accurately predict unknown masses is crucial.

Since Weizsäcker first proposed the liquid-drop model nuclear mass formula in 1935 [28], various types of nuclear mass formulas have been proposed, including the macroscopic model (e.g., Bethe–Weizsäcker (BW) models [28–30]), microscopic model (e.g., Skyrme Hartree–Fock–Bogoliubov (HFB) models [31–33]

This work was supported by the Ministry of Science and Technology of China (No. 2022YFE0103400), Natural Science Foundation of Guangxi Province (No. 2021GXNSFAA196052), and National Natural Science Foundation of China (No. 11965004).

✉ Li Ou
liou@gxnu.edu.cn

1 College of Physics and Technology, Guangxi Normal University, Guilin 541004, China

2 Guangxi Key Laboratory of Nuclear Physics and Technology, Guangxi Normal University, Guilin 541004, China

and relativistic mean-field (RMF) model [34]), macroscopic–microscopic models (e.g., finite-range droplet model (FRDM) [35, 36], Weizsäcker–Skyrme (WS) model [37–41], Koura–Tachibana–Uno–Yamada (KTUY) model [42], Duflo–Zuker model (DZ) [43], etc.), systematic local mass Garvey–Kelson relation [44], and Audi–Wapstra extrapolation method [26, 27, 45–47]. These nuclear mass formulas can reproduce the known nuclear masses with a certain accuracy, but their predictions appear to diverge as the isospin asymmetry increases, particularly for unknown masses. For details on the introduction and comparison of these models, refer to [48] and the references therein. Therefore, a more accurate nuclear mass formula requires more accurate experimental data, particularly for extremely neutron-rich nuclei, and a deeper understanding of the nuclear force, particularly the isospin symmetry breaking from theory. However, efforts have been made to improve the precision and extrapolation ability of nuclear mass models using machine learning algorithms [49–53].

The macroscopic–microscopic mass model can systematically and quickly calculate the mass of nuclei on the entire nuclide chart with a high accuracy and good prediction ability. In this paper, the properties of drip-line nuclei are studied using the WS nuclear mass formula (WS3.3) [38], and the nuclear Coulomb energy is studied using the mass relations of mirror nuclei. The remainder of this paper is structured as follows: Sect. 2 briefly introduces the WS3.3 nuclear mass formula. The properties of drip-line nuclei based on the WS3.3 formula and the Coulomb energy based on the mass relations of mirror nuclei are presented in Sect. 3 and 4, respectively. Finally, a summary is given in Sect. 5.

2 WS3.3 nuclear mass formula

The WS nuclear mass formula is based on the Bathe–Weizsäcker liquid-drop model [30] and Skyrme energy density functional theory. The evolution of the model and a detailed introduction are presented in [37–41]. The WS3.3 version is adopted in this paper. In the WS nuclear mass formula, the macroscopic part of the binding energy of the nucleus considers the correction of the deformation based on the liquid-drop model, and the microscopic part is the shell-correction energy. Considering the deformed liquid-drop and shell-correction energies, the total energy of the nucleus can be expressed as follows:

$$E(A, Z, \beta) = E_{\mathrm{LD}}(A, Z) \prod_{k \geqslant 2} (1 + b_k \beta_k^2) + \Delta E(A, Z, \beta), \tag{1}$$

where $E_{\mathrm{LD}}(A, Z)$ represents the conventional spherical nuclear liquid-drop energy as stipulated by the modified Bath–Bethe–Weizsäcker mass formula, and b_k reflects the correction of the liquid-drop energy owing to nuclear deformation. The spherical nuclear liquid-drop energy is predominantly composed of five components: volume, surface, Coulomb, symmetry, and pairing energies.

$$E_{\mathrm{LD}}(A, Z) = a_{\mathrm{v}} A + a_{\mathrm{s}} A^{2/3} + E_{\mathrm{c}} + a_{\mathrm{sym}} I^2 A + a_{\mathrm{pair}} A^{-1/3} \delta_{\mathrm{np}}, \tag{2}$$

with an isospin asymmetry of $I = \frac{N-Z}{A}$. The Coulomb energy term is expressed as

$$E_{\mathrm{c}} = a_{\mathrm{c}} \frac{Z^2}{A^{1/3}} (1 - Z^{-2/3}). \tag{3}$$

The Coulomb exchange energy, surface dispersion effect, and self-energy are all represented by the $Z^{-2/3}$ term. Additionally, based on the traditional liquid-drop model, the surface symmetry energy term of the finite nucleus and an isospin correction term are introduced to describe the Wigner effect of nuclei [35, 54]:

$$a_{\mathrm{sym}} = c_{\mathrm{sym}} \left[1 - \frac{\kappa}{A^{1/3}} + \frac{2 - |A|}{2 + |I| A} \right]. \tag{4}$$

The correction of this term for the nuclear binding energy is

$$E_{\mathrm{w}} = c_{\mathrm{sym}} I^2 A \left[\frac{2 - |A|}{2 + |I| A} \right] \approx 2 c_{\mathrm{sym}} |I| - c_{\mathrm{sym}} |I|^2 + \cdots . \tag{5}$$

δ_{np} can be expressed as [55]

$$\delta_{\mathrm{np}} = \begin{cases} 2 - |I| & \text{for even } N \text{ and even } Z \\ |I| & \text{for odd } N \text{ and odd } Z \\ 1 - |I| & \text{for even } N \text{ and odd } Z, N > Z \\ 1 - |I| & \text{for odd } N \text{ and even } Z, N < Z \\ 1 & \text{for even } N \text{ and odd } Z, N < Z \\ 1 & \text{for odd } N \text{ and even } Z, N > Z \end{cases}. \tag{6}$$

In WS3.3, the macroscopic energy of deformed nuclei is obtained by correcting the nuclear deformation on the macroscopic binding energy of spherical nuclei. The terms with b_k in Eq. (1) describe the contribution of nuclear deformation (including β_2, β_4, and β_6) to E_{LD}. The mass dependence of the curvature b_k is expressed as [37]

$$b_k = \left(\frac{k}{2} \right) g_1 A^{1/3} + \left(\frac{k}{2} \right)^2 g_2 A^{-1/3}, \tag{7}$$

according to the Skyrme energy density functional calculation, which significantly reduces the computation time for calculations for deformed nuclei [37].

The microscopic shell correction of the binding energy is obtained using the traditional Strutinsky shell-correction method [56]:

$$\Delta E = c_1 E_{\mathrm{sh}} + |I| E'_{\mathrm{sh}}. \tag{8}$$

Here c_1 represents the scale factor used to adjust the proportions of the macroscopic and microscopic shell-correction parts to the total binding energy. E_{sh} and E'_{sh} denote the shell-correction energy of a nucleus and its corresponding mirror nucleus, respectively. The term $|I|E'_{\mathrm{sh}}$ is introduced to account for the mirror constraint from isospin symmetry, resulting in a 10% reduction in the root-mean-square (RMS) deviation of the nuclear mass calculations.

The calculation of the single-particle energy levels of a nucleus based on the deformed Woods–Saxon potential, combined with microscopic shell correction, requires four parameters: the potential well depth parameter V_0, radius parameter r_0, surface dispersion parameter a, and spin-orbit coupling parameter λ_0. With nine parameters in the macroscopic part, the WS3.3 model has a total of 13 parameters. The parameters in the model shown in Table 1 are determined by fitting the experimental data from 2149 nuclei with N and $Z \geqslant 8$ in AME2003. With this set of improved WS3.3 parameters, the RMS deviation of the nuclear mass calculated for 2149 nuclei is 0.441 MeV. Additionally, the RMS deviations of the neutron separation energies for 1988 nuclei and 46 superheavy nuclei are 0.332 and 0.263 MeV, respectively.

3 Properties of the drip-line nucleus

The drip-line nucleus is a nucleus whose separation energy of the last neutron or proton is less than zero. The drip line can be obtained by marking these nuclei in the nuclide chart, and it serves as the boundary for the existence of nuclei in the nuclide chart. When the drip line is crossed, the binding energy of the nucleus is insufficient to bind the last nucleon. Consequently, the near-drip-line nucleus exhibits extremely weak binding, resulting in a significantly more important proportion of coupling between nucleus-bound states and the continuum spectrum. This phenomenon causes many peculiarities among the nuclei near the drip line, such as the neutron skin and neutron halo [57, 58], cluster structure [59], and the emergence and disappearance of traditional magic numbers [60, 61]. Owing to their very low separation energies, the accurate prediction of drip-line positions requires high accuracy in nuclear mass formulas. Note that the differences in the nuclear masses given by the various models increase as the deviation from the β-stable valley increases. Therefore, the properties related to the drip line and drip-line nuclei serve as important standards for testing nuclear mass formulas.

Table 1 Parameters of the WS3.3 mass model

Parameter	Value	Parameter	Value
a_v (MeV)	−15.6223	V_0 (MeV)	−46.8784
a_s (MeV)	18.0571	r_0 (fm)	1.3840
a_c (MeV)	0.7194	a (fm)	0.7842
c_{sym} (MeV)	29.1563	λ_0	26.3163
κ	1.3484	g_1	0.00895
a_{pair}(MeV)	−5.4423	g_2	−0.46324
c_1	0.62966		

First, the masses of the nuclei are calculated, and the drip, β-stable, and most bound nucleus (MBN) lines are determined using the WS3.3 nuclear mass formula, as shown in Fig. 1. The MBN is identified as the nucleus with the maximum specific binding energy in each isotope chain, whereas the β-stable nucleus has the maximum specific binding energy in each isobar chain. Nuclei with known experimental masses and mirror nuclei are obtained from the AME2020 mass table.

The isospin asymmetry of the β-stable nucleus, drip-line nucleus, and MBN as functions of the neutron number given by the WS3.3 model is shown in Fig. 2. Separate representations of odd and even charges are provided for the drip-line nuclei to mitigate the influence of the symmetry effect. These results show that in the light nucleus region, both β-stable nuclei and MBN exhibit essentially similar isospin asymmetry, which increase as the neutron number increases because the Coulomb repulsion must be offset by excess neutrons. Furthermore, the isospin asymmetry of most β-stable nuclei progressively exceed those of the MBN. In light nuclear regions, the isospin asymmetry of the proton drip-line nucleus tends to be smaller than zero, indicating a proton-rich state. However, this tendency shifts toward increasing values, aligning more closely with those exhibited by the MBN as the neutron number increases. Conversely, as a natural consequence, the isospin asymmetry displayed by neutron drip-line nuclei significantly surpass those observed in β-stable nuclei, MBNs, and proton drip-line nuclei. As the nucleus size increases, the isospin asymmetry of the

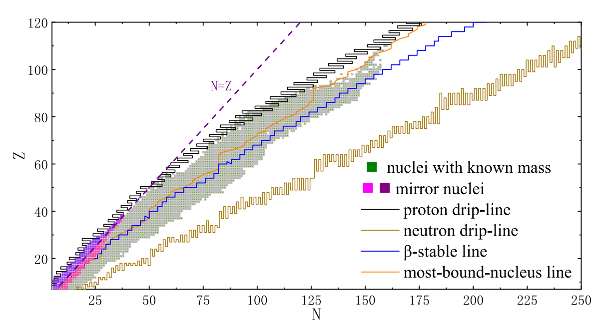

Fig. 1 (Color online) Nuclide chart with the β-stable, MBN, proton drip, and neutron drip lines predicted using the WS3.3 model and the nuclei from the AME2020 mass table

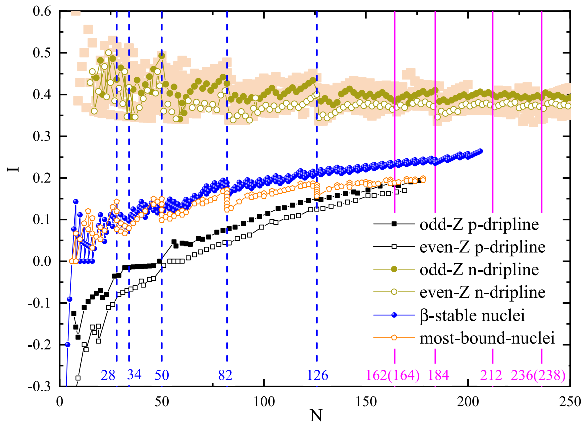

Fig. 2 (Color online) Isospin asymmetry of the β-stable nucleus, neutron drip-line nucleus, and MBN as a function of neutron number given by the WS3.3 model. The blue dashed lines denote the locations of traditional magic numbers: 28, 34, 50, 82, and 126. The magenta solid lines denote the locations where the isospin asymmetries of the neutron drip-line nucleus saltation of 162 (164), 184, 212, and 236 (238). The pink block area denotes the isospin asymmetry of the neutron drip-line nucleus given by some nuclear mass models

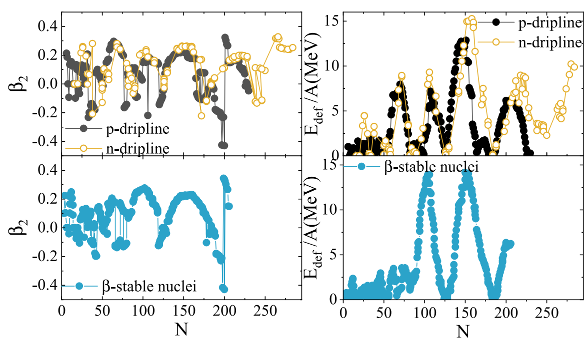

Fig. 3 (Color online) Quadrupole deformation values (left) and deformation energies (right) of β-stable and drip-line nuclei as a function of the neutron number using the WS3.3 model

neutron drip-line nucleus tends to decrease, eventually saturating at approximately 0.38 in the heavy nuclei region. Some nuclear mass models, such as HFB27 [33], RMF [34], FRDM12 [36], KTUY [42], DZ31 [43], and Bhagwat [62] also predict the same tendency, as shown by the pink block in Fig. 2. This suggests that the increased Coulomb energy of the heavy drip-line nucleus, resulting from the increased number of protons, is not simply offset by a further increase in the neutron number.

To elucidate the mechanism for equilibrating the binding energy of heavy drip-line nuclei, we analyze the quadrupole deformation and deformation energy of the nucleus as a function of the neutron number, as presented in Fig. 3. The deformation energy is defined as the difference between the energies of the deformed and conventional spherical nuclei [6]:

$$E_{\text{def}} = E(0) - E(\beta_{\text{gs}}), \tag{9}$$

where β_2, β_4, and β_6 are considered in the calculations. Taking ^{238}U as an example, for a spherical nucleus, $E(0) = -1790.958$ MeV for a deformed nucleus with $\beta_2 = 0.213$, $\beta_4 = 0.069$, and $\beta_6 = -0.003$, $E(\beta_2) = -1799.423$, $E(\beta_{2,4}) = -1801.964$, and $E(\beta_{2,4,6}) = -1801.972$ MeV, respectively. $E_{\text{def}} = 11.014$ MeV.

We can observe that the β_2 distribution of the proton drip-line nucleus closely resembles that of β-stable nuclei throughout the nuclear region, ranging from -0.3 to 0.3. Similarly, the β_2 distribution of the neutron drip-line nucleus is relatively uniform in the regions where $N < 200$. This implies that these nuclei can counterbalance the increased Coulomb repulsion owing to charge enhancement through symmetry energy by enriched neutrons and deformation energy by suitable deformation. Conversely, in the region where $N > 200$ for the neutron drip-line nucleus, no nucleus has a small deformation ($\beta_2 \in [-0.1, 0.1]$). The strong deformation results in a large deformation energy for the heavy nuclei on the neutron drip line, as shown in the right-hand panel of Fig. 3. A comparison of the results shown in Fig. 2 reveals that, for heavy nucleus at the neutron drip line, heightened Coulomb energy owing to augmented charge cannot be mitigated completely by symmetry energy with insufficient neutrons but is resisted complementally by strong nuclear deformations.

Furthermore, a clear correlation between isospin asymmetry of nucleus at the neutron drip line and magic number is observed in Fig. 2. In Fig. 2, the blue dotted lines denote the positions of traditional magic numbers: 28, 34, 50, 82, and 126, which precisely correspond to locations where saltation occurs simultaneously in isospin asymmetry of the MBN and that of neutron drip-line nucleus with odd Z and even Z. This correlation is not apparent in the proton drip-line nucleus. Nevertheless, no confirmed magic number corresponds to some saltation positions in the heavy nuclei region. This implies that the neutron numbers corresponding to these positions, i.e., 162 (164), 184, 212, and 236 (238), denoted by magenta lines, might also be neutron magic numbers. To obtain a more distinct perspective on the correlation between the isospin asymmetry of the neutron drip-line nucleus and the magic number, Fig. 4 presents the differences in proton numbers between two neighboring nuclei at the neutron drip line ΔZ as a function of the neutron number. We can imagine that, without the shell effect, the proton number should change smoothly with the neutron number. However,

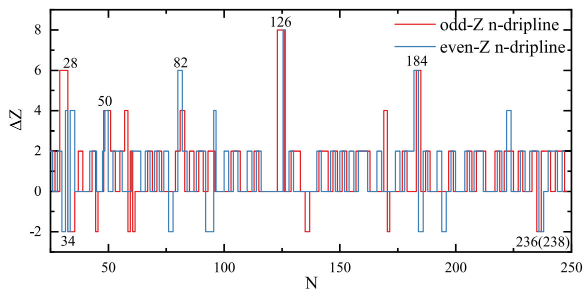

Fig. 4 (Color online) Differences in proton numbers between two neighboring nuclei at the neutron drip line

Fig. 4 shows that for some nuclei, with the addition of two neutrons, the proton number increases by −2, 4, 6, even 8. This indicates a shell effect.

The positions where ΔZ of the neutron drip-line nucleus with odd Z and even Z simultaneously undergo saltation nearby are 28, 34, 50, 82, 126, 184, and 236 (238). They reproduce known magic numbers (28, 34, 50, 82, and 126) quite well. The neutron numbers 184 and 236 (238) may be new magic numbers. Using shell model calculations, 184 [63–74] and 238 [63, 66] are also predicted as new neutron magic numbers. In addition, 162 [63, 69, 70, 73] and 164 [63, 69] are predicted as new neutron numbers, which are predicted using isospin asymmetry saltation but not by the charge number saltation in this paper. This indicates that the saltations in the isospin asymmetry of the neutron drip-line nucleus and in the difference in proton numbers between two neighboring nuclei at the neutron drip line can be used as criteria to verify the prospective magic number.

4 Mass relation of mirror nuclei

A pair of nuclei with the same mass number A and, exchanged proton number Z and neutron number N are called mirror nuclei. With symmetric properties, mirror nuclei are widely used to study nuclear structures [75–78] and reactions [79–82].

Based on the isospin symmetry of nuclear interactions, the binding energy difference between mirror nuclei (BEDbMN) results from the Coulomb energy and small mass difference between the neutron and proton [83, 84]. Precise measurement of the masses of mirror nuclei enables the study of isospin symmetry and the charge independence of the nuclear force and can be employed to test nuclear structure models. It is an effective approach for enhancing the precision of nuclear mass formulas by utilizing the mass relations of mirror nuclei to investigate the nuclear mass formula, particularly the reasonable correction of the Coulomb term [38, 85–93].

By subtracting the Coulomb energy, the nuclear force-dependent part in the BEDbMN can be considered approximately equal, i.e.,

$$E_{\mathrm{B}} - E_{\mathrm{C}} \approx E'_{\mathrm{B}} - E'_{\mathrm{C}}, \tag{10}$$

where E_{B} represents the total energy of the nucleus, E_{C} represents the Coulomb energy of the nucleus, and E'_{B} and E'_{C} represent the correlation values of the corresponding mirror nuclei. By combining the macroscopic–microscopic mass formula with the equation above, we can obtain the constraint between the shell corrections of mirror nuclei,

$$|\Delta E - \Delta E'| \approx 0. \tag{11}$$

This implies that the difference in the shell-correction energies between one pair of mirror nuclei should be small. Considering the $|I|E'_{\mathrm{sh}}$ term in Eq. (8), we can obtain

$$|\Delta E - \Delta E'| = (c_1 - |I|)|E_{\mathrm{sh}} - E'_{\mathrm{sh}}|. \tag{12}$$

The $|I|E'_{\mathrm{sh}}$ term is useful for restoring the isospin symmetry in the mirror nuclei and can effectively reduce the shell-correction deviation $|\Delta E - \Delta E'|$ in pairs of mirror nuclei, which is required by the constraint in Eq. (10). With the $(c_1 - |I|)$ term, $|\Delta E - \Delta E'|$ is generally less than 2 MeV in WS3.3 [38]. We can imagine that although $E_{\mathrm{sh}} \neq E'_{\mathrm{sh}}$ by the shell correction using the Strutinsky method, $|\Delta E - \Delta E'|$ can be closer to zero to satisfy the constraint in Eq. (11) with more isospin symmetry in the mirror nuclei being restored.

Because the nuclear force is independent of the charge of the nucleus, the BEDbMN is only reflected in the Coulomb energy terms. Therefore, the Coulomb term coefficient can be determined using the BEDbMN. Considering the Coulomb exchange effect, the Coulomb term in (3) can be expressed as follows:

$$E_{\mathrm{c}} = \frac{a_{\mathrm{c}} Z^2}{A^{1/3}}(1 - cZ^{-2/3}). \tag{13}$$

When $c = 1.0$, this indicates the WS3.3 parameter. With Eq. (13), the BEDbMN can be presented as

$$\Delta E = \frac{a_{\mathrm{c}}}{A^{1/3}}(Z_1^2 - Z_2^2) + \frac{c \cdot a_{\mathrm{c}}}{A^{1/3}}(Z_2^{4/3} - Z_1^{4/3}). \tag{14}$$

Tian et al. specified a_{c} and c by fitting a BEDbMN with $11 \le A \le 75$ in the AME2016 mass table [94]. In this paper, a_{c} and c are determined by fitting the BEDbMN with $Z, N \ge 6$ in the AME2003 mass table. The following results are calculated for nuclei with $Z, N \ge 6$ unless otherwise stated. The three sets of Coulomb term coefficients and RMS deviations of the theoretical BEDbMN from the experimental data are listed in Table 2. A comparison between the theoretical BEDbMN and experimental data is presented in Fig. 5. The results show that the Coulomb term coefficient

Table 2 Three sets of the Coulomb term coefficient and RMS deviations for the BEDbMN calculated from the experimental data

	a_c (MeV)	c	σ (MeV) (AME2003)	σ (MeV) (AME2020)
This work	0.73	1.49	0.312	0.334
Tian	0.69	1.19	0.418	0.453
WS3.3	0.71	1.0	0.684	0.816

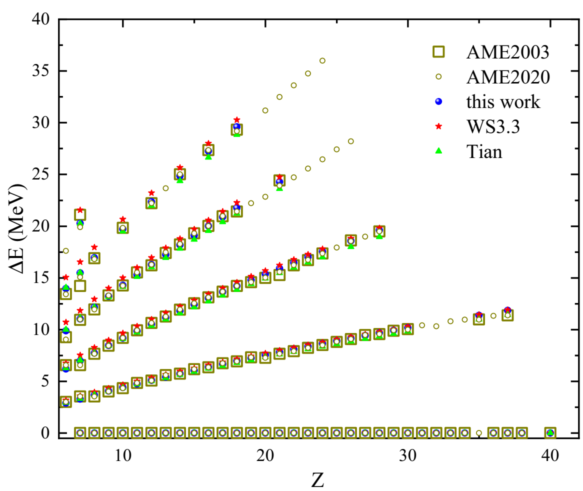

Fig. 5 (Color online) Comparison of the experimental data and BEDbMN calculated using the three sets of empirical parameters

in this paper yields the smallest RMS deviation for the calculated BEDbMN from the experimental data. Even with 21 pairs of newly added mirror nuclei and some nuclear masses corrected in the AME2020 mass table, compared with AME2003, the RMS deviation in this study is minimal. Figure 5 shows that the BEDbMN as a function of charge number is divided into several groups. If the second term in the expression for the BEDbMN pair Eq. (14) is disregarded, it can be represented as

$$\Delta E = \frac{a_c}{A^{1/3}}(Z_1^2 - Z_2^2) + \mathcal{O}(Z_1, Z_2). \tag{15}$$

From $Z_1 = A - N_1 = A - Z_2 = N_2$, we obtain

$$\Delta E = a_c\,(N - Z)A^{2/3} + \mathcal{O}(N, Z). \tag{16}$$

Thus, ΔE is grouped by $N - Z$ and is proportional to $A^{2/3}$ with a slope of $a_c(N - Z)$ and an intercept of $\mathcal{O}(N, Z)$. By fitting the BEDbMN pair by group, we can express the empirical expressions for $N - Z = 1, 2, 3, 4$ as

$$\begin{aligned} \Delta E &= E_0 + bA^{2/3}, \\ b &= 0.76428(N - Z) - 0.04435, \\ E_0 &= -0.63154(N - Z) - 0.21727(N - Z)^2. \end{aligned} \tag{17}$$

The BEDbMNs newly added to AME2020 also fall within the results provided by the empirical formula. This suggests that the empirical formula can be employed to estimate the unmeasured mass of the nucleus with high precision if the mass of its mirror pair has already been measured experimentally.

Because only one pair of mirror nuclei has $N - Z = 5$ (^{19}Mg and ^{19}N) in the AME2003 mass table, a linear fit is not feasible. The empirical curve for $N - Z = 5$ shown in Fig. 6 is an extrapolation of expression (17). An apparent variation in the experimental value for mirror nulei pair of ^{19}Mg and ^{19}N between AME2003 and AME2020 can be observed. This is because a correction of 1.2 MeV is applied to the binding energy of ^{19}Mg. With this correction and one new mirror nuclei pair (^{17}C and ^{17}Na) added to AME2020, the extrapolated result for $N - Z = 5$ corresponds with the data of AME2020.

Compared with AME2003, the masses of 21 new mirror nuclei pairs are included in the AME2020 mass table, which can be utilized to verify the accuracy of the mirror nuclei binding energy difference formula. The RMS deviations between the experimental and theoretical masses for the 21 newly added mirror nuclei pairs in this work and the WS3.3 model are shown in Table 3. Considering the mass relations of the mirror nuclei, the mass formula generates a lower RMS deviation. Currently, proton-rich nuclei whose masses have been measured are considerably close to the proton drip line; however, some nuclei remain to be synthesized and

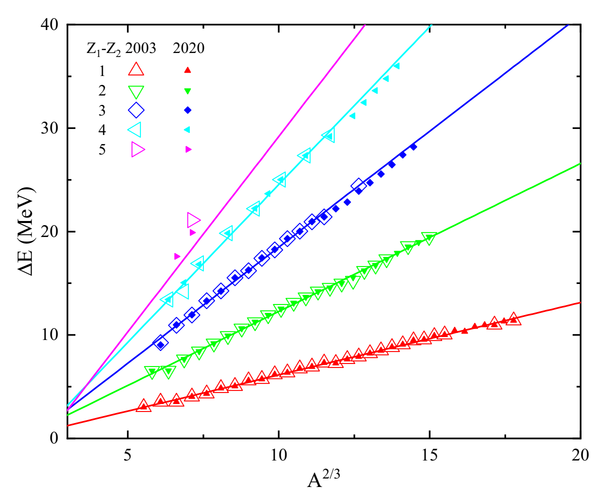

Fig. 6 (Color online) Comparison of the experimental data and binding energy differences of mirror nucleus pair calculated by the empirical parameters

Table 3 RMS deviations of BEDbMNs between experimental and theoretical values for 21 newly added mirror nuclei pairs in this work, the WS3.3 model, and some other models

	a_c (MeV)	c	σ (MeV)
This work	0.73	1.49	0.378
WS3.3 [38]	0.71	1.0	0.825
HFB27 [33]			0.446
RMF [34]			0.618
FRDM12 [36]			0.441
KTUY [42]			0.395

measured. More accurate predictions of the experimentally unmeasured masses of mirror nuclei toward the proton drip line by employing the mass relation of the mirror nuclei would be beneficial.

The study of the BEDbMN reveals that a more precise Coulomb term, particularly the Coulomb exchange term coefficient, can be acquired from a BEDbMN. In addition, the nuclear mass formula has a better physical basis. Therefore, we attempt to utilize three schemes in the nuclear mass formula to refit the AME2003 mass table and investigate the effect of the Coulomb exchange term on the accuracy of the nuclear mass formula.

A. The Coulomb term coefficients a_c and c are fixed by taking the values determined from the mass relations of mirror nuclei. The other 12 parameters are determined via the optimization method.
B. The Coulomb exchange term coefficient c assumes different values, the other 13 parameters, including a_c, are determined using the optimization method. Specifically, the WS3.3 parameter is obtained when $c = 1.0$.
C. The Coulomb term coefficients a_c and c and the other 14 parameters are determined using the optimization method.

The values of the Coulomb term coefficients for the three schemes and their mass RMS deviations are listed in Table 4. Although Scheme A provided the most accurate description of the binding energy difference for 71 pairs of mirror nuclei, the RMS deviation of the mass of 2149 nuclei is larger than that provided by the WS3.3 parameter set. As shown in Scheme B, the Coulomb exchange term coefficient ranges from 0 to 2.0, and the Coulomb direct term coefficient a_c varies only slightly. This result indicates that the Coulomb direct term coefficient is robust against the Coulomb exchange term coefficient. The mass RMS deviation as a function of the Coulombic exchange coefficient is shown in Fig. 7. The RMS deviation is the smallest when $c \simeq 1$. This precisely matches the exchange term coefficient adopted in WS3.3. Additionally, the results of Scheme C

Table 4 Values of the Coulomb term coefficient using various schemes and their mass RMS deviations

Scheme	c	a_c (MeV)	σ (MeV)
A	1.49	0.730	0.489
	1.00	0.719	0.440
B	2.00	0.730	0.571
	1.49	0.724	0.474
	1.20	0.721	0.445
	1.00	0.719	0.440
	0.90	0.718	0.443
	0.80	0.717	0.448
	0.50	0.714	0.481
	0.00	0.712	0.600
C	1.02	0.720	0.440
HFB27 [33]			0.533
RMF [34]			2.0675
FRDM12 [36]			0.5812
KTUY [42]			0.653

show that the optimal Coulomb coefficients given by the nuclear mass formula with the addition of one adjustable parameter are nearly indistinguishable from the results of WS3.3, and virtually no improvement occurs in accuracy.

The preceding discussion reveals that the accuracy of the nuclear mass formula is not enhanced but rather diminishes when directly using the Coulomb term coefficients determined by the mass relations of mirror nuclei pairs. A possible reason for this is that 71 pairs of mirror nuclei constitute a relatively small proportion of the 2149 nuclei, and no mirror nuclei exist in the heavy nuclei region. The Coulomb term coefficient determined by the mirror nuclei in the light nuclei region based on the local mass relation is less precise when extrapolated to the heavy nuclei region. As a test, the above three schemes are employed to calculate the masses of

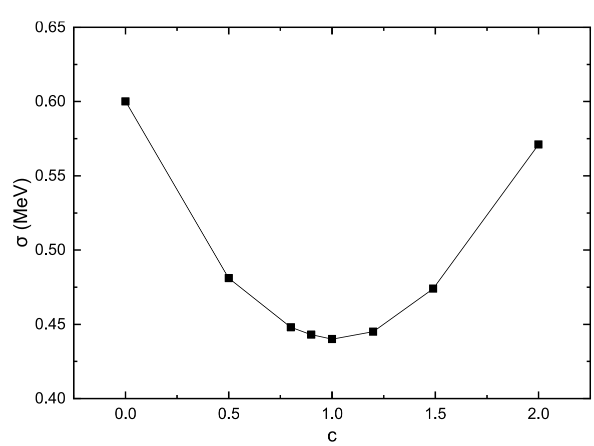

Fig. 7 Mass RMS deviation as a function of the Coulomb exchange coefficient

Table 5 Values of the Coulomb term coefficient and RMS deviations of masses obtained by fitting mirror nuclei mass in AME2003 with different schemes

Scheme	c	a_c (MeV)	σ (MeV)	Comment
A	1.49	0.730	0.629	This work
	1.00	0.719	0.620	WS3.3
B	1.49	0.763	0.657	
	1.00	0.730	0.625	
C	0.312	0.663	0.588	
HFB27 [33]			0.871	
RMF [34]			1.577	
FRDM12 [36]			1.110	
KTUY [42]			0.728	

71 pairs of mirror nuclei, and the obtained RMS deviations are presented in Table 5.

Similar to the results based on the 2149 nuclei optimization parameters, the RMS deviation obtained by the method in this paper remains higher than that of WS3.3 parameters, although the disparity in RMS deviations between the two methods is not significant. The accuracy of the result for $c = 1.0$ is still higher than that for $c = 1.49$. Although the accuracy of Scheme C is slightly improved, the Coulomb coefficient determined by mirror nuclei masses differs significantly from that determined by the 2149 nuclear masses, and the experimental data of the 2149 nuclear masses cannot be well represented using the coefficients in Scheme C. These observations suggest a systematic correlation among the terms of the nuclear mass formula. An improvement in the accuracy of a single term in the formula, such as the Coulomb term, may not enhance the accuracy of the entire nuclear mass formula.

Finaly, let us consider the Coulomb exchange coefficient $c = 1.49$ obtained by fitting the BEDbMN in this study. The well-known Fermi gas model yields a considerably smaller result of 0.76 (that is, $\frac{5}{4}\left(\frac{3}{2\pi}\right)^{2/3}$), which is only half the value herein. This can be explained by the simplified Coulomb energy term, i.e., Eq. (13), adopted in this work. A more sophisticated Coulomb energy form is [91, 95]

$$E_c^f = E_c^d + E_c^e + E_c^s = \frac{3}{5}\frac{e^2}{r_0}\frac{Z^2}{A^{1/3}}\left[1 - \frac{5}{4}\left(\frac{3}{2\pi}\right)^{2/3} Z^{-2/3} - Z^{-1}\right], \tag{18}$$

the first term E_c^d is the direct term, the second term E_c^e is called the exchange term in the Fermi gas model, and the third term E_c^s is called the self-energy term and equals the total Coulomb energy of Z protons moving individually in a sphere which has the same size as the nucleus in consideration. If the self-energy effect is considered as a correlation of the exchange term, the Coulomb energy can be expressed as shown in Eq. (13), which is the form adopted in this work.

The Coulomb energies of the β-stable nuclei, calculated using various Coulomb energy forms, are presented in Fig. 8. As shown in the figure, E_c with $c = 0.76$ can reproduce E_c^f with the direct and exchange terms, and E_c with $c = 1.0$ can reproduce E_c^f using the direct, exchange, and self-energy terms. If surface dispersion is considered, the Coulomb energy should be further suppressed with ΔE_c^{sd}; here ΔE_c^{sd} is the difference in the Coulomb energy between nuclei with and without surface dispersion. The nuclear density distribution was determined by the restricted density variational method using the Skyrme energy density functional. We observe that E_c with $c = 1.49$ can completely reproduce the Coulomb energy, including the direct, exchange, and self-energy terms, with surface dispersion effects being considered.

5 Summary

The properties of the drip-line nucleus and mass relation of mirror nuclei are studied based on the WS3.3 nuclear mass formula. We observe that the isospin asymmetry of heavy nuclei on the neutron drip line tends toward a saturation value of 0.38. An analysis of the nuclear quadrupole deformation value β_2 and the deformation energy as a function of the neutron number suggests that in the heavy nuclei region, the strong Coulomb energy caused by the augmented proton is resisted by enormous deformation but not by the further addition of neutrons because of isospin asymmetry saturation. Additionally, the conventional magic number has a distinct correspondence with the saltation position of the isospin asymmetries of the MBN, the difference in proton numbers between two neighboring

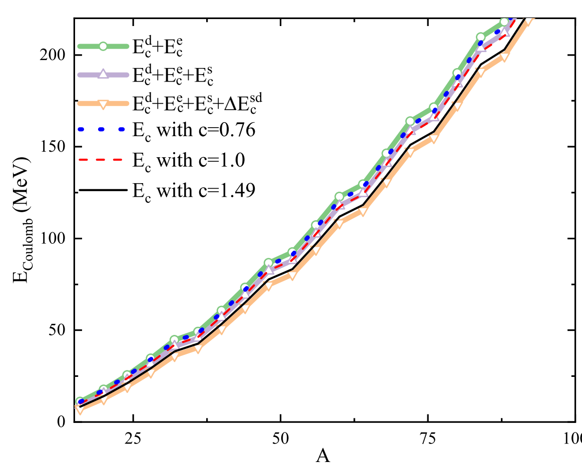

Fig. 8 (Color online) Coulomb energies for the β-stable nucleus with various Coulomb energy forms

nuclei at the neutron drip line, and isospin asymmetry degree at the neutron drip-line nucleus as a function of the neutron number. Therefore, saltation without a known corresponding magic number can serve as a reference to verify the undetermined neutron magic number.

By considering the mass relation of mirror nuclei, i.e., BEDbMN, a Coulomb term with a stronger physical foundation and greater accuracy is obtained. However, the accuracy of the mass formula with the BEDbMN considered is lower than that without the BEDbMN considered. A reason for this is that the Coulomb term coefficients are determined based on insufficient experimental data of mirror nuclei with $A < 75$, which are insufficient to describe the entire mass table globally. The other reason is that a systematic relationship exists between the coefficients in the mass formula; we should not expect it to improve accuracy by improving some of the coefficients independently. However, the relation of the BEDbMN can be used to accurately determine the mass of one of the mirror nuclei, which is experimentally unknown, by another whose mass is known. This is particularly useful for predicting the mass of isotopes that are difficult to synthesize or measure experimentally toward a proton drip line for $N < 50$ where a mirror nuclei pair exists.

Acknowledgements The authors thank Tao Li at Guangxi Normal University for assistance with calculations.

Author contributions All authors contributed to the study conception and design. Material preparation, data collection, and analysis were performed by Meng-Ting Wan, Li Ou, and Ning Wang. The first draft of the manuscript was written by Men-Ting Wan, and all authors commented on the previous versions of the manuscript. All authors read and approved the final manuscript.

Data availability The data that support the findings of this study are openly available in Science Data Bank at https://cstr.cn/31253.11.sciencedb.18300 and https://www.doi.org/10.57760/sciencedb.18300.

Declarations

Conflict of interest The authors declare that they have no conflict of interest.

References

1. D. Lunney, J.M. Pearson, C. Thibault, Recent trends in the determination of nuclear masses. Rev. Mod. Phys **75**, 1021 (2003). https://doi.org/10.1103/RevModPhys.75.1021
2. A. de Roubin, D. Atanasov, K. Blaum et al., Nuclear deformation in the $A \approx 100$ region: comparison between new masses and mean-field predictions. Phys. Rev. C **96**, 014310 (2017). https://doi.org/10.1103/PhysRevC.96.014310
3. Y. Kun, X.R. Zhou, J.W. Cui et al., Effect of time-odd fields on odd-even mass differences of semi-magic nuclei. Sci. China Phys. Mech. Astron **59**, 652002 (2016). https://doi.org/10.1007/s11433-016-5796-6
4. F. Wienholtz, D. Beck, K. Blaum et al., Masses of exotic calcium isotopes pin down nuclear forces. Nature **498**, 346 (2013). https://doi.org/10.1038/nature12226
5. P.H. Ćwiok, W. Heenen, Nazarewicz, shape coexistence and triaxiality in the superheavy nuclei. Nature **433**, 705 (2005). https://doi.org/10.1038/nature03336
6. A. Sobiczewski, K. Pomorski, Description of structure and properties of superheavy nuclei. Prog. Part. Nucl. Phys **58**, 292 (2007). https://doi.org/10.1016/j.ppnp.2006.05.001
7. A. Sobiczewski, Theoretical description of the decay chain of the nucleus ^{294} 118. J. Phys. G Nucl. Part. Phys **43**, 095106 (2016). https://doi.org/10.1088/0954-3899/43/9/095106
8. Y.T. Oganessian, V.K. Utyonkov, Superheavy nuclei from ^{48} Ca-induced reactions. Nucl. Phys. A **944**, 62 (2015). https://doi.org/10.1088/0954-3899/43/9/095106
9. Q.H. Mo, M. Liu, N. Wang, Systematic study of shell gaps in nuclei. Phys. Rev. C **90**, 024320 (2014). https://doi.org/10.1103/PhysRevC.90.024320
10. S. Michimasa, M. Kobayashi, Y. Kiyokawa, Magic nature of neutrons in ^{54}Ca: first mass measurements of $^{55-57}$Ca. Phys. Rev. Lett **121**, 022506 (2018). https://doi.org/10.1103/PhysRevLett.121.022506
11. M. Rosenbusch, P. Ascher, D. Atanasov, Probing the N=32 shell closure below the magic proton number Z=20: mass measurements of the exotic Isotopes ^{52,53}K. Phys. Rev. Lett **121**, 202501 (2015). https://doi.org/10.1103/PhysRevLett.114.202501
12. E. Leistenschneider, M.P. Reiter, S. Ayet San Andres et al., Dawning of the $N = 32$ shell closure seen through precision mass measurements of neutron-rich titanium isotopes. Phys. Rev. Lett **121**, 062503 (2018). https://doi.org/10.1103/PhysRevLett.120.062503
13. J. Dobaczewski, W. Nazarewicz, T.R. Werner et al., Mean-field description of ground-state properties of drip-line nuclei: pairing and continuum effects. Phys. Rev. C **53**, 2809 (1996). https://doi.org/10.1103/PhysRevC.53.2809
14. L. Gaudefroy, W. Mittig, N.A. Orr et al., Direct mass measurements of ^{19}B, ^{22}C, ^{29}F, ^{31}Ne, ^{34}Na and other light exotic nuclei. Phys. Rev. Lett **109**, 202503 (2012). https://doi.org/10.1103/PhysRevLett.109.202503
15. J. Erler, N. Birge, M. Kortelainen et al., The limits of the nuclear landscape. Nature **486**, 509 (2012). https://doi.org/10.1038/nature11188
16. S.G. Zhou, Study on superheavy nuclei and superheavy elements. Nucl. Phys. Rev **34**, 318 (2017). https://doi.org/10.11804/NuclPhysRev.34.03.318
17. W. Nazarewicz, The limits of nuclear mass and charge. Nature Phys **14**, 5 (2018). https://doi.org/10.1038/s41567-018-0163-3
18. E. Minaya Ramirez, D. Ackermann, K. Blaum et al., Direct mapping of nuclear shell effects in the heaviest elements. Science **337**, 1207 (2012). https://doi.org/10.1126/science.1225636
19. R.N. Wolf, D. Beck, K. Blaum et al., Plumbing neutron stars to new depths with the binding energy of the exotic nuclide Zn 82. Phys. Rev. Lett **110**, 041101 (2013). https://doi.org/10.1103/PhysRevLett.110.041101
20. H. Schatz, S. Gupta, P. Möller et al., Strong neutrino cooling by cycles of electron capture and β-decay in neutron star crusts. Nature **505**, 62 (2014). https://doi.org/10.1038/nature12757
21. Y. Qian, G. Wasserburg, Where, oh where has the r-process gone? Phys. Rep **442**, 237 (2007). https://doi.org/10.1016/j.physrep.2007.02.006
22. M. Arnould, S. Goriely, K. Takahashi, The r-process of stellar nucleosynthesis: astrophysics and nuclear physics achievements and mysteries. Phys. Rep **450**, 97 (2007). https://doi.org/10.1016/j.physrep.2007.06.002

23. Z. Li, Z.M. Niu, B.H. Sun, WLW mass model in nuclear r-process calculations. Acta Phys. Sin **61**, 072601 (2012). https://doi.org/10.7498/aps.61.072601
24. B. Franzke, H. Geissel, G. Münzenberg, Mass and lifetime measurements of exotic nuclei in storage rings. Mass Spectrom. Rev **27**, 428 (2008). https://doi.org/10.1002/mas.20173
25. B.H. Sun, Yu.A. Litvinov, I. Tanihata et al., Toward precision mass measurements of neutron-rich nuclei relevant to r-process nucleosynthesis. Front. Phys **10**, 102102 (2015). https://doi.org/10.1002/mas.20173
26. M. Wang, W.J. Huang, F.G. Kondev et al., The AME 2020 atomic mass evaluation (II). Tables, graphs and references. Chin. Phys. C **45**, 030003 (2021). https://doi.org/10.1088/1674-1137/abddaf
27. W.J. Huang, M. Wang, F.G. Kondev et al., The AME 2020 atomic mass evaluation (I). Evaluation of input data, and adjustment procedures. Chin. Phys. C **45**, 030002 (2021). https://doi.org/10.1088/1674-1137/abddb0
28. C.V. Weizsäcker, Zur theorie der kernmassen. Zeitschrift für Physik **96**(7), 431–458 (1935). https://doi.org/10.1007/BF01337700
29. M.W. Kirson, Mutual influence of terms in a semi-empirical mass formula. Nucl. Phys. A **798**, 29 (2008). https://doi.org/10.1016/j.nuclphysa.2007.10.011
30. H.A. Bethe, R.F. Bacher, *Nuclear physics A* (Rev. Mod. Phys, Stationary states of nuclei, 1936). https://doi.org/10.1103/RevModPhys.8.82
31. S. Goriely, M. Samyn, J.M. Pearson, Further explorations of Skyrme-Hartree-Fock-Bogoliubov mass formulas. VII. Simultaneous fits to masses and fission barriers. Phys. Rev. C **75**, 064312 (2007). https://doi.org/10.1103/PhysRevC.75.064312
32. S. Goriely, N. Chamel, J.M. Pearson, Skyrme-Hartree-Fock-Bogoliubov nuclear mass formulas: crossing the 0.6 MeV accuracy threshold with microscopically deduced pairing. Phys. Rev. Lett **102**, 152503 (2009). https://doi.org/10.1103/PhysRevLett.102.152503
33. S. Goriely, N. Chamel, J.M. Pearson, Hartree-Fock-Bogoliubov nuclear mass model with 0.50 MeV accuracy based on standard forms of Skyrme and pairing functionals. Phys. Rev. C **88**, 061302 (2013). https://doi.org/10.1103/PhysRevC.88.061302
34. L. Geng, H. Toki, J. Meng, Masses, deformations and charge radii-nuclear ground-state properties in the relativistic mean field model. Prog. Theo. Phys **113**, 785 (2005). https://doi.org/10.1143/PTP.113.785
35. P. Möller, J.R. Nix, W.D. Myers et al., Nuclear ground-state masses and deformations. At. Data Nucl. Data Tables **59**, 185 (1995). https://doi.org/10.1006/adnd.1995.1002
36. P. Möller, A.J. Sierk, T. Ichikawa et al., Nuclear ground-state masses and deformations: FRDM(2012). At. Data Nucl. Data Tables **109–110**, 1 (1996). https://doi.org/10.1016/j.adt.2015.10.002
37. N. Wang, M. Liu, X.Z. Wu, Modification of nuclear mass formula by considering isospin effects. Phys. Rev. C **81**, 044322 (2010). https://doi.org/10.1103/PhysRevC.81.044322
38. N. Wang, Z.Y. Liang, M. Liu et al., Mirror nuclei constraint in nuclear mass formula. Phys. Rev. C **82**, 044304 (2010). https://doi.org/10.1103/PhysRevC.82.044304
39. N. Wang, M. Liu, Nuclear mass predictions with a radial basis function approach. Phys. Rev. C **84**, 051303 (2011). https://doi.org/10.1103/PhysRevC.84.051303
40. M. Liu, N. Wang, Y.G. Deng et al., Further improvements on a global nuclear mass model. Phys. Rev. C **84**, 014333 (2011). https://doi.org/10.1103/PhysRevC.84.014333
41. N. Wang, M. Liu, X.Z. Wu et al., Surface diffuseness correction in global mass formula. Phys. Lett. B **734**, 215 (2014). https://doi.org/10.1016/j.physletb.2014.05.049
42. H. Koura, T. Tachibana, M. Uno et al., Nuclidic mass formula on a spherical basis with an improved even-odd term. Prog. Theor. Phys **113**, 305 (2005). https://doi.org/10.1143/PTP.113.305
43. J. Duflo, A.P. Zuker, Microscopic mass formulas. Phys. Rev. C **52**, R23 (1995). https://doi.org/10.1103/10.1103/PhysRevC.52.R23
44. G.T. Garvey, W.J. Gerace, R.L. Jaffe et al., Set of nuclear-mass relations and a resultant mass table. Rev. Mod. Phys **41**, S1 (1969). https://doi.org/10.1103/RevModPhys.41.S1
45. G. Audi, A.H. Wapstra, C. Thibault, The Ame 2003 atomic mass evaluation. Nucl. Phys. A **729**, 337 (2003). https://doi.org/10.1016/j.nuclphysa.2003.11.003
46. W.J. Huang, G. Audi, M. Wang et al., The AME2016 atomic mass evaluation (I). Evaluation of input data; and adjustment procedures. Chin. Phys. C **41**, 030002 (2017). https://doi.org/10.1088/1674-1137/41/3/030002
47. M. Wang, G. Audi, F.G. Kondev et al., The AME 2016 atomic mass evaluation (II). Tables, graphs and references. Chin. Phys. C **41**, 030003 (2017). https://doi.org/10.1088/1674-1137/41/3/030003
48. T. Yamaguchi, H. Koura, Yu.A. Litvinov et al., Masses of exotic nuclei. Prog. Part. Nucl. Phys **120**, 103882 (2021). https://doi.org/10.1016/j.ppnp.2021.103882
49. Z.M. Niu, H.Z. Liang, Nuclear mass predictions based on Bayesian neural network approach with pairing and shell effects. Phys. Lett. B **778**, 48 (2018). https://doi.org/10.1016/j.physletb.2018.01.002
50. Z.M. Niu, H.Z. Liang, Nuclear mass predictions with machine learning reaching the accuracy required by r-process studies. Phys. Rev. C **106**, L021303 (2022). https://doi.org/10.1103/PhysRevC.106.L021303
51. X.H. Wu, Y.Y. Lu, P.W. Zhao, Multi-task learning on nuclear masses and separation energies with the kernel ridge regression. Phys. Lett. B **834**, 137394 (2022). https://doi.org/10.1016/j.physletb.2022.137394
52. Z. Gao, Y.J. Wang, H.L. Lü et al., Machine learning the nuclear mass. Nucl. Sci. Tech **32**, 109 (2021). https://doi.org/10.1007/s41365-021-00956-1
53. Z. Gao, Q. Li (2023) Studies on several problems in nuclear physics by using machine learning. Nucl. Tech. **46**, 95. https://doi.org/10.11889/j.0253-3219.2023.hjs.46.080009(in Chinese)
54. W. Satuła, D.J. Dean, J. Gary et al., On the origin of the Wigner energy. Phys. Lett. B **407**, 103 (1997). https://doi.org/10.1016/S0370-2693(97)00711-9
55. J. Mendoza-Temis, J.G. Hirsch, A.P. Zuker, The anatomy of the simplest Duflo-Zuker mass formula. Nucl. Phys. A **843**, 14 (2010). https://doi.org/10.1016/j.nuclphysa.2010.05.055
56. V.M. Strutinsky, F.A. Ivanjuk, A new definition of shell corrections to the liquid drop energy. Nucl. Phys. A **225**, 405 (1975). https://doi.org/10.1016/0375-9474(75)90688-0
57. I. Tanihata, H. Savajols, R. Kanungo, Recent experimental progress in nuclear halo structure studies. Prog. Part. Nucl. Phys **68**, 215 (2013). https://doi.org/10.1016/j.ppnp.2012.07.001
58. A. Trzcińska, J. Jastrzębski, P. Lubiński, Recent experimental progress in nuclear halo structure studies. Phys. Rev. Lett **87**, 082501 (2001). https://doi.org/10.1103/PhysRevLett.87.082501
59. W. Vonoertzen, M. Freer, Y. Kanadaenyo, Nuclear clusters and nuclear molecules. Phys. Rep **432**, 43 (2006). https://doi.org/10.1016/j.physrep.2006.07.001
60. I. Tanihata, Nuclear structure studies from reaction induced by radioactive nuclear beams. Prog. Part. Nucl. Phys **35**, 505 (1995). https://doi.org/10.1016/0146-6410(95)00046-L
61. O. Sorlin, M.G. Porquet, Nuclear magic numbers: new features far from stability. Prog. Part. Nucl. Phys. Supp **61**, 602 (2008). https://doi.org/10.1016/j.ppnp.2008.05.001
62. A. Bhagwat, Simple nuclear mass formula. Phys. Rev. C **90**, 064306 (2014). https://doi.org/10.1103/PhysRevC.90.064306

63. J. Meng, H. Toki, S.G. Zhou et al., Relativistic continuum Hartree Bogoliubov theory for ground-state properties of exotic nuclei. Prog. Part. Nucl. Phys **57**, 470 (2006). https://doi.org/10.1016/j.ppnp.2005.06.001
64. J.J. Li, W.H. Long, J. Margueron et al., Superheavy magic structures in the relativistic Hartree-Fock-Bogoliubov approach. Phys. Lett. B **732**, 169 (2014). https://doi.org/10.1016/j.physletb.2014.03.031
65. A.A. Saldanha, A.R. Farhan, M.M. Sharma, Superheavy nuclei with the vector self-coupling of the ω-meson in relativistic mean-field theory. J. Phys. G Nucl. Part. Phys **36**, 115103 (2009). https://doi.org/10.1088/0954-3899/36/11/115103
66. W. Zhang, J. Meng, S.Q. Zhang et al., Magic numbers for superheavy nuclei in relativistic continuum Hartree-Bogoliubov theory. Nucl. Phys. A **753**, 106 (2005). https://doi.org/10.1016/j.nuclphysa.2005.02.086
67. S.G. Nilsson, C.F. Tsang, A. Sobiczewski et al., On the nuclear structure and stability of heavy and superheavy elements. Nucl. Phys. A **131**, 1 (1969). https://doi.org/10.1016/0375-9474(69)90809-4
68. U. Mosel, W. Greiner, On the stability of superheavy nuclei against fission. Z. Physik **222**, 261 (1969). https://doi.org/10.1007/BF01392125
69. P. Möller, J.R. Nix, Stability of heavy and superheavy elements. J. Phys. G Nucl. Part. Phys **20**, 1681 (1994). https://doi.org/10.1088/0954-3899/20/11/003
70. Z. Patyk, A. Sobiczewski, Ground-state properties of the heaviest nuclei analyzed in a multidimensional deformation space. Nucl. Phys. A **533**, 132 (1991). https://doi.org/10.1016/0375-9474(91)90823-O
71. K. Rutz, M. Bender, T. Bürvenich, Superheavy nuclei in self-consistent nuclear calculations. Phys. Rev. C **56**, 238 (1997). https://doi.org/10.1103/PhysRevC.56.238
72. M. Bender, K. Rutz, P.-G. Reinhard, Shell structure of superheavy nuclei in self-consistent mean-field models. Phys. Rev. C **60**, 034304 (1999). https://doi.org/10.1103/PhysRevC.60.034304
73. S. Ćwiok, J. Dobaczewski, P.-H. Heenen et al., Shell structure of the superheavy elements. Nucl. Phys. A **611**, 211 (1996). https://doi.org/10.1016/S0375-9474(96)00337-5
74. G.A. Lalazissis, M.M. Sharma, P. Ring et al., Superheavy nuclei in the relativistic mean-field theory. Nucl. Phys. A **608**, 202 (1996). https://doi.org/10.1016/0375-9474(96)00273-4
75. C.W. Ma, Y.D. Song, H.L. Wei et al., Binding energies of near proton-drip line $Z = 22 - 28$ isotopes determined from measured isotopic cross section distributions. Sci. China Phys. Mech. Astron **62**, 012013 (2019). https://doi.org/10.1007/s11433-018-9256-8
76. N. Wang, T. Li et al., Shell and isospin effects in nuclear charge radii. Phys. Rev. C **88**, 011301(R) (2013). https://doi.org/10.1103/PhysRevC.88.011301
77. R. An, S. Sun, L.G. Cao, Constraining nuclear symmetry energy with the charge radii of mirror pair nuclei. Nucl. Sci. Tech **34**, 119 (2023). https://doi.org/10.1007/s41365-023-01269-1
78. S. Zhang, Y. Geng, F. Xu, Ab initio Gamow shell-model calculations for dripline nuclei.(in Chinese) Nucl. Tech. **46**, 121 (2023). https://doi.org/10.11889/j.0253-3219.2023.hjs.46.080012
79. C.W. Ma, X.X. Chen, X.B. Wei et al., Systematic behavior of fragments in Bayesian neural network models for projectile fragmentation reactions. Phys. Rev. C **108**, 044606 (2023). https://doi.org/10.1103/PhysRevC.108.044606
80. B. Guo, Z.H. Li, X.X. Bai et al., Determination of the astrophysical ^{26}Si$(p,\gamma)^{27}$P reaction rate from the asymptotic normalization coefficients of ^{27}Mg $\rightarrow$ 26Mg $+ n$. Phys. Rev. C **73**, 048801 (2006). https://doi.org/10.1103/PhysRevC.73.048801
81. J. Lee, X.X. Xu, K. Kaneko et al., Large isospin asymmetry in ^{22}Si/^{22}O mirror gamow-teller transitions reveals the halo structure of ^{22}Al. Phys. Rev. Lett **125**, 0192503 (2020). https://doi.org/10.1103/PhysRevLett.125.192503
82. L. Yang, C.J. Lin, H.M. Jia, et al., Progress on nuclear reactions and related nuclear structure at low energies. Nucl. Tech. **46**, 080006 (2023). https://doi.org/10.11889/j.0253-3219.2023.hjs.46.080006 (in Chinese)
83. S. Shlomo, Nuclear coulomb energies. Rep. Prog. Phys **41**, 957 (1978). https://doi.org/10.1088/0034-4885/41/7/001
84. W.E. Ormand, Mapping the proton drip line up to A = 70. Phys. Rev. C **55**, 2407 (1997). https://doi.org/10.1103/PhysRevC.55.2407
85. M. Bao, Y. Lu, Y.M. Zhao et al., Simple relations between masses of mirror nuclei. Phys. Rev. C **94**, 044323 (2016). https://doi.org/10.1103/PhysRevC.94.044323
86. Y.Y. Zong, C. Ma, M.Q. Lin et al., Mass relations of mirror nuclei for both bound and unbound systems. Phys. Rev. C **152**, 034321 (2022). https://doi.org/10.1103/PhysRevC.105.034321
87. C. Xu, M. Bao, Improved mass relations of mirror nuclei. Nucl. Sci. Tech **35**, 157 (2024). https://doi.org/10.1007/s41365-024-01501-6
88. John M. Blatt, Victor F. Weisskopf, *Theoretical Nuclear Physics* (Springer-Verlag, New York, 1979)
89. J.L. Tian, N. Wang, C. Li et al., Improved Kelson-Garvey mass relations for proton-rich nuclei. Phys. Rev. C **87**, 014313 (2013). https://doi.org/10.1103/PhysRevC.87.014313
90. Y.Y. Zong, M.Q. Lin, M. Bao et al., Mass relations of corresponding mirror nuclei. Phys. Rev. C **100**, 054315 (2019). https://doi.org/10.1103/PhysRevC.100.054315
91. Y.Y. Zong, C. Ma, Y.M. Zhao et al., Mass relations of mirror nuclei. Phys. Rev. C **102**, 024302 (2020). https://doi.org/10.1103/PhysRevC.102.024302
92. C. Ma, Y.Y. Zong, Y.M. Zhao et al., Mass relations of mirror nuclei. Phys. Rev. C **102**, 024330 (2020). https://doi.org/10.1103/PhysRevC.102.024330
93. Y.H. Zhang, P. Zhang, X.H. Zhou et al., Isochronous mass measurements of $T_z = -1 fp$-shell nuclei from projectile fragmentation of ^{58}Ni. Phys. Rev. C **98**, 014319 (2018). https://doi.org/10.1103/PhysRevC.98.014319
94. J.L. Tian, D. Yuan, Y.Y. Cui et al., Nuclear mass parabola and its applications. Chin. Phys. C **43**, 124104 (2019). https://doi.org/10.1088/1674-1137/43/12/124104
95. J.A. Nolen, J.P. Schiffer, Coulomb energies. Annu. Rev. Nucl. Sci **19**, 471 (1969). https://doi.org/10.1146/annurev.ns.19.120169.002351